This is a repository copy of *Temperature and band gap dependence of GaAsBi p-i-n diode current–voltage behaviour*.

White Rose Research Online URL for this paper:
http://eprints.whiterose.ac.uk/171783/

Article:

PAPER • OPEN ACCESS

Temperature and band gap dependence of GaAsBi p-i-n diode current–voltage behaviour

IOP ebooks™

Bringing together innovative digital publishing with leading authors from the global scientific community.

Start exploring the collection−download the first chapter of every title for free.

IOP Publishing

Journal of Physics D: Applied Physics

Temperature and band gap dependence of GaAsBi p-i-n diode current–voltage behaviour

R D Richards[iD], F Harun, M R M Nawawi, Y Liu[iD], T B O Rockett[iD] and J P R David

University of Sheffield, Sheffield, South Yorkshire S1 3JD, United Kingdom

E-mail: R.Richards@Sheffield.ac.uk

CrossMark

Abstract

The dark current characteristics of two series of bulk GaAsBi p-i-n diodes are analysed as functions of temperature and band gap. Each temperature dependent measurement indicates that recombination current dominates in these devices. The band gap dependence of the dark currents is also consistent with recombination dominated current for the devices grown at a common growth temperature, indicating that the presence of Bi does not directly adversely affect the dark currents. However, the devices grown at different growth temperatures exhibit a faster increase in dark current with decreasing device band gap, suggesting that a reduced growth temperature causes a reduction in minority carrier lifetime.

Keywords: GaAsBi, devices, diodes, highly mismatched alloys, molecular beam epitaxy, temperature dependence

(Some figures may appear in colour only in the online journal)

1. Introduction

GaAsBi and its alloys have shown significant potential in recent years for a number of optoelectronic device applications such as mid-infrared photosensitive detectors, infrared emitters, telecommunication lasers, photoconductive terahertz antennas, spintronic devices and multijunction photovoltaics [1–5]. Compared with indium (In) or antimony (Sb) alloys of GaAs, Bi diminishes the bandgap with a considerably smaller increase in the lattice constant; it causes approximately 75 meV/% Bi reduction of the bandgap [1]. This is potentially useful, for example, for multiple-quantum well based photovoltaics, where the critical thickness of InGaAs necessitates the use of complex, interlayered structures to achieve

long wavelength absorption [6]. The main cause of the band gap reduction is a rapid raising of the valence band due to an anti-crossing interaction with Bi induced localised states [7], which also causes an increase in the spin-orbit splitting. When the spin-orbit splitting becomes larger than the band gap (around 10% Bi), it may be possible to supress the CHSH (hot hole producing) Auger recombination process, which potentially could increase the efficiency of mid-infrared lasers [1].

Considerable attention has been paid to the molecular beam epitaxy (MBE) growth conditions necessary to incorporate significant Bi fractions into GaAs, with up to 22% incorporation achieved using low growth temperatures and low As to Ga flux ratios [8]. This kind of unconventional growth regime can lead to the formation of anti-site defects and Bi clusters [9–11], whose effect on GaAsBi diode characteristics is, as yet, unclear.

There have been relatively few reports of GaAsBi based diode dark current characteristics [3, 12–19] despite this being a key aspect of device performance. For reference, there have also been some reports of the dark currents observed

in devices containing other dilute bismide materials: InAsBi [20], GaSbBi [21], and InGaAsBi [22]. The material quality of GaAsBi is known to be affected by the surfactant effect of Bi [23] and strain relaxation [24], and the optical properties are influenced by the presence of localised states near the valence band edge caused by valence band hybridisation with Bi induced localised states [25–27]. The influences of temperature and alloy composition on dark current behaviour are key to understanding the current mediation mechanisms in GaAsBi and for the development of GaAsBi devices at particular Bi fractions, for example the >10% [Bi] required for suppression of Auger recombination in GaAsBi lasers [1], or the ~2.5%–6% required for photovoltaics [2, 28]. Some results have shown that growth conditions and Bi content both influence the dark current behaviour [17, 18], but these have been limited to room temperature characteristic comparisons.

In this paper the current–voltage characteristics of two series of bulk GaAsBi p-i-n diodes are investigated at temperatures between ~20 °C (~293 K) and 120 °C (~393 K). The results are related to the diffusion and recombination mediated current behaviours as laid out in the Shockley diode equation and used to determine the impact of bismuth content and growth conditions on the dark current characteristics in GaAsBi.

2. Experimental

This paper describes the analysis of two series of bulk double heterojunction p-i-n diodes (illustrated in figure 1). For one series (referred to as the T_{grow} series) the Bi flux (F_{Bi}) was kept constant for each diode's GaAsBi region and the GaAsBi growth temperature for each device was different; for the other series (referred to as the F_{Bi} series) the GaAsBi growth temperature was kept constant and the Bi flux was varied throughout the series. The key, device specific growth and structural parameters are shown in table 1. All *i*-regions are approximately 100 nm thick.

All devices were grown using an Omicron scanning tunnelling microscope-MBE (STM-MBE) machine, operating as a standard MBE machine, using *n*+ GaAs (100) substrates. Following standard outgassing and oxide removal procedures a Si doped GaAsBi buffer layer was deposited at 580 °C. The substrate temperature was then reduced to the GaAsBi growth temperature (see table 1) during a 20 min growth pause. The GaAsBi was deposited continuously under a near-stoichiometric As$_4$ flux to provide a wider As flux window for Bi incorporation [30]; As$_2$ was used during the growth of the rest of the device. The GaAsBi growth was immediately followed by a thin GaAs layer in an effort to prevent subsequent Bi segregation. Following the GaAsBi region growth, the growth temperature was raised to approximately 580 °C during another 20 min growth pause for growth of the Be doped GaAs capping layers. This means that the GaAsBi regions experienced an *in situ* anneal at 580 °C for approximately 1 h. More detailed information on sample growth and estimated Bi contents can be accessed elsewhere [18].
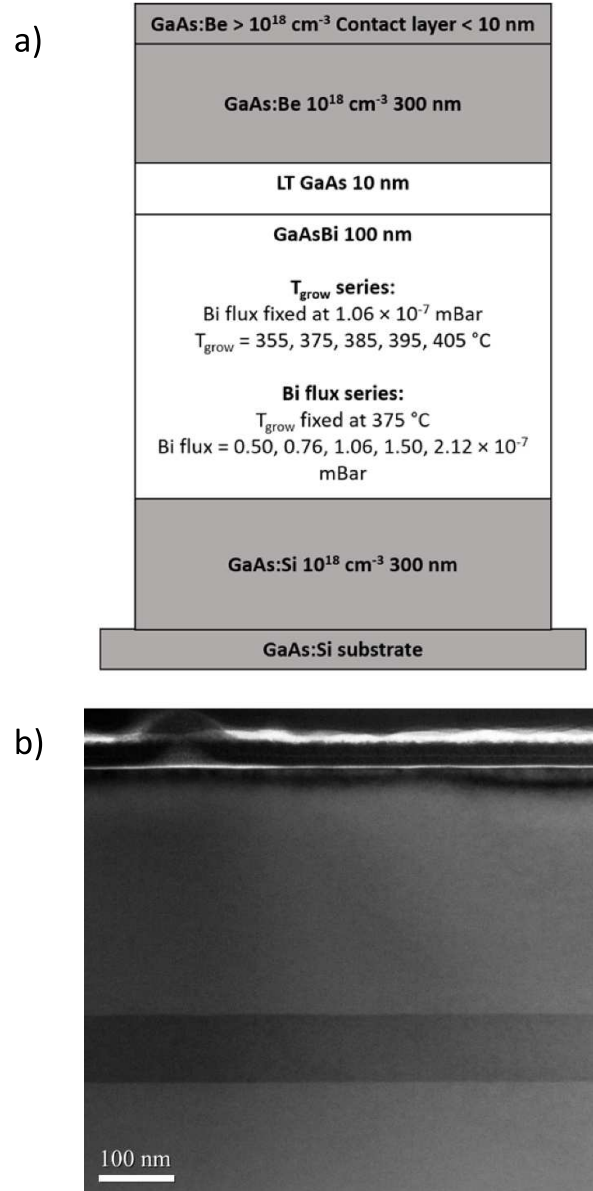
Figure 1. (a) Schematic diagram of the device structures in this work. (b) Bright field TEM image of the device grown under the lowest Bi flux. The growth direction is vertically upwards.

Following growth, the diodes were fabricated into circular mesa devices of several radii up to 200 μm using standard photolithography techniques and wet etching. The back, *n*-type contact comprised In/Ge/Au and the top, *p*-type contact comprised Au/Zn/Au. Annular top contacts were deposited to allow optical access to the device.

J–V measurements were taken using a Keithley source measure unit in a dark room. The devices were heated on a copper heating block and their temperature was estimated using a thermocouple placed nearby the device within the copper block. For each of the measurements discussed in this paper, several devices of different radii were measured to ensure that the absolute current values scaled with device area.

Selected diodes were imaged by transmission electron microscopy (TEM); for these measurements, specimens were

Table 1. Growth and structural details of the devices. Note that the T_{grow} and F_{Bi} series contain a common sample, which is indicated in bold. The F_{Bi} values are quoted as the ion gauge readings of the Bi beam equivalent pressure used during GaAsBi growth.

Series	T_{grow} (°C)	F_{Bi} ($\times 10^{-7}$ mBar)	[Bi] (%) from XRD [18]	E_g (eV) inferred from [Bi] following [29]
T_{grow}	355	1.06	3.5	1.16
	375	**1.06**	**3.3**	**1.18**
	385	1.06	2.8	1.21
	395	1.06	2.2	1.25
	405	1.06	1.4	1.31
F_{Bi}	375	0.50	1.3	1.31
	375	0.76	2.3	1.25
	375	**1.06**	**3.3**	**1.18**
	375	1.50	4.1	1.12
	375	2.12	5.4	1.05
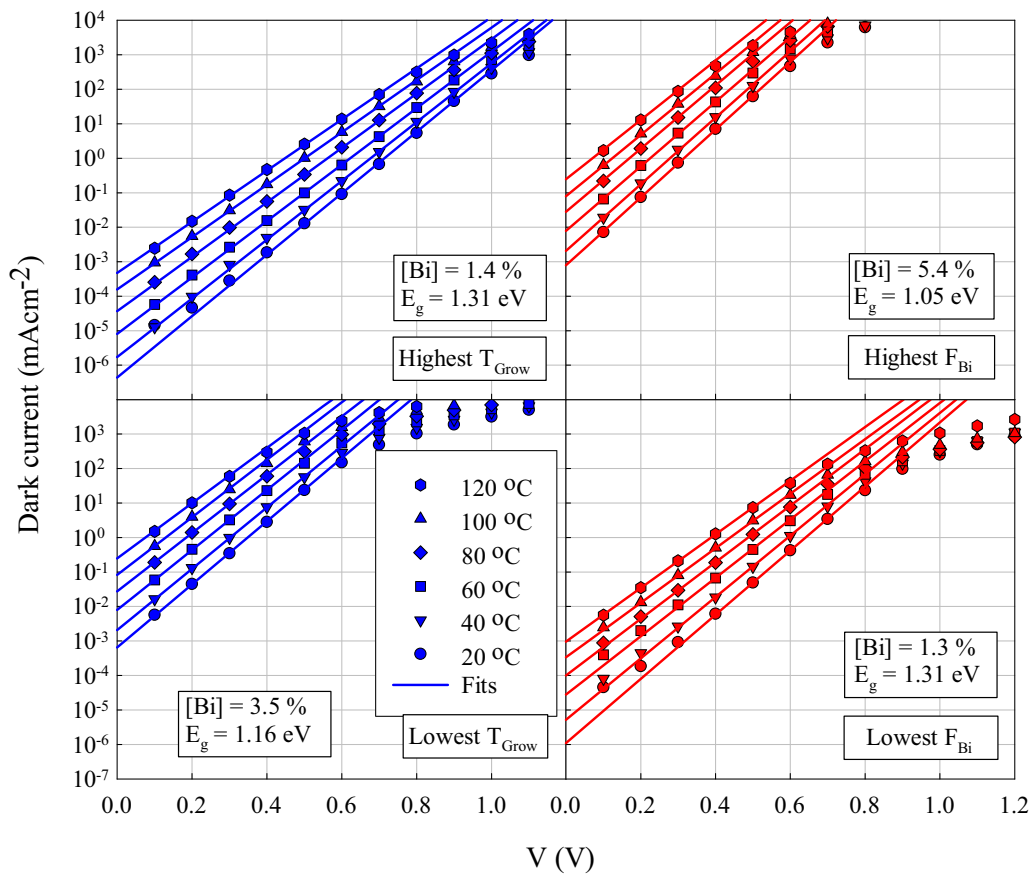
Figure 2. *J*–*V* curves from selected diodes. The solid fitting lines are based on equation (1) and are extrapolated back to the *y*-axis to indicate the saturation current density (J_0) values. The results from the T_{grow} series are shown in blue, while those from the F_{Bi} series are shown in red.

prepared parallel to 110 using standard methods and examined in a JEOL 2000FX TEM operating at 200 kV. Magnification was calibrated to <0.5% using a superlattice structure with period measured by x-ray diffraction (XRD) to an accuracy better than 0.1%.

3. Theory

The current voltage characteristic of an ideal diode at a given temperature is described by the Shockley diode equation [31]:

$$J = q\sqrt{\frac{D}{\tau}}\frac{n_i^2}{N}\exp\left[\frac{qV}{k_BT}\right] + \frac{qW_Dn_i}{2\tau}\exp\left[\frac{qV}{2k_BT}\right] - J_L$$

$$\approx J_0\left[\exp\left(\frac{qV}{nk_BT}\right) - 1\right] - J_L \qquad (1)$$

where *J* is the total current density passing through the diode, *q* is the charge on an electron, *D* and τ are the diffusion coefficient and the recombination lifetime of the minority carriers in the junction, n_i is the intrinsic carrier density, *N* is the minority carrier impurity concentration, *V* is the applied bias, k_B is the Boltzmann constant, *T* is the diode's temperature, W_D is
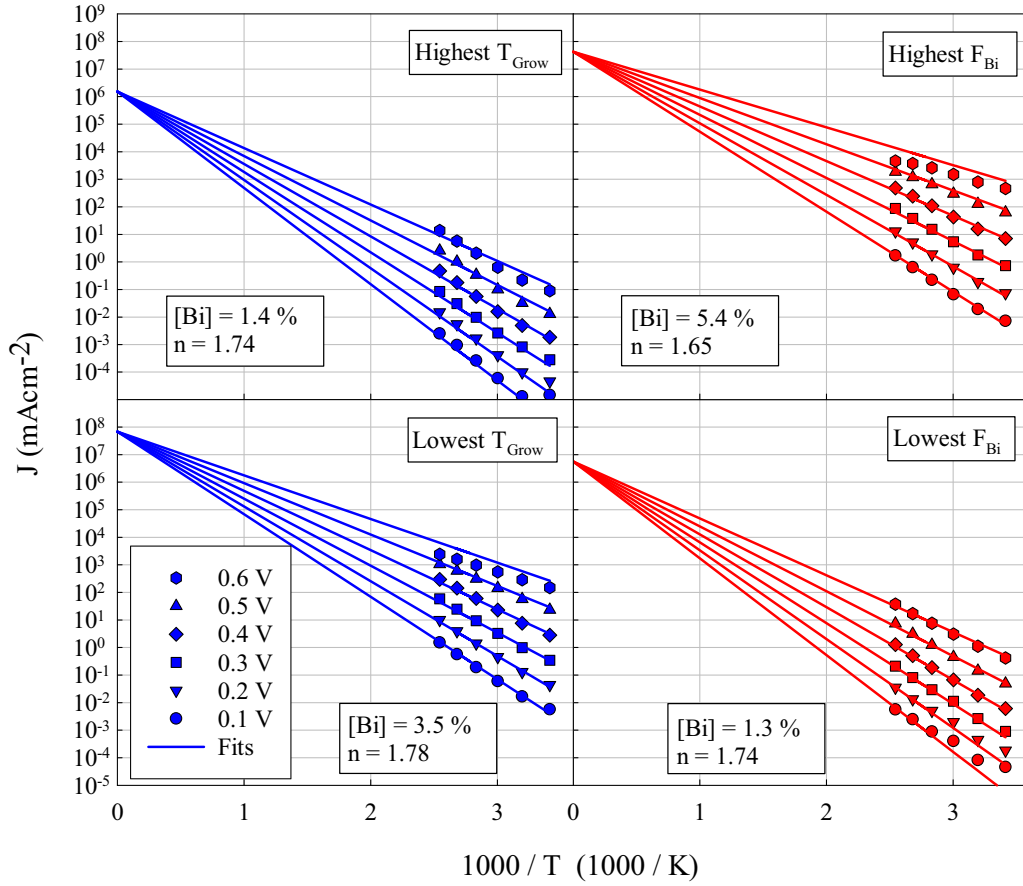
Figure 3. Arrhenius plots of the *J*–*V* data for selected diodes. For each device, the fitting lines were all produced using the band gap determined from the XRD results in [18] and a fixed ideality factor as displayed in the figure.

the depletion width, J_L is the additional drift current density due to illumination, J_0 is the diode's saturation current density, and n is the diode's ideality factor. The ideality factor describes the balance of contributions to the total current from diffusion current (if dominant then $n = 1$) and recombination current (if dominant then $n = 2$). In reality, the value of n is unlikely to reach 2 even for recombination dominated current, as the assumptions made in calculating that value rarely hold true in a real device [32].

The intrinsic carrier density is approximately given by:

$$n_i = 4.9 \times 10^{15} \left(\frac{m_{de} m_{dh}}{m_0^2} \right)^{3/4} M_C^{1/2} T^{3/2} \exp\left(\frac{-E_g}{2k_B T} \right) \quad (2)$$

where m_{de} (m_{dh}) is density of states effective mass for electrons (holes), m_0 is the electron rest mass, h is Planck's constant, M_C is the number of equivalent minima in the conduction band.

Grouping all non- or weakly-temperature dependent terms into simple coefficients (A', B' and C') and assuming no illumination, the temperature dependence of J can be approximated by:

$$J \approx A' \underbrace{\left[T^3 \exp\left(\frac{qV - E_g}{k_B T} \right) \right]}_{\text{Diffusion current}} + B' \underbrace{\left[T^{1.5} \exp\left(\frac{qV - E_g}{2k_B T} \right) \right]}_{\text{Recombination current}}$$

$$\approx C' \left[\exp\left(\frac{qV - E_g}{n k_B T} \right) \right]. \quad (3)$$

For each diode the fractional change of the band gap in the temperature range of this experiment was assumed to be small in comparison with the fractional changes of T and V, so the band gap was assumed to be constant and was inferred from the XRD measurements of the Bi contents in [18], using the methodology in [29].

4. Results and discussion

Figure 2 shows the *J*–*V* curves of diodes grown under the highest and lowest growth temperatures and the highest and lowest Bi fluxes. For each device at each temperature, the data is fitted with equation (1) to yield values for J_0 and n. The fitting achieved for these devices is representative of the quality of each fitting. Not all devices were measured at elevated tem-
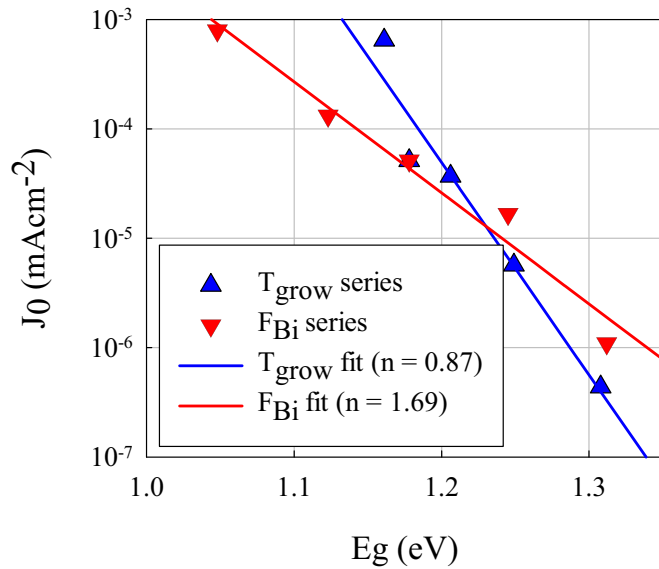
Figure 4. Room temperature saturation current density data from the diodes at room temperature. The red line has been fitted to the F_{Bi} series data (red); this line represents an ideality factor of 1.69. The blue line is fitted to the T_{grow} series data (blue); this line represents an ideality factor of 0.87.

peratures. At high bias, the current is lower than predicted, which would normally be ascribed to parasitic series resistance, but in this case the data cannot be fit by assuming series resistance at high bias. A similar effect has been seen in other reports on GaAsBi diodes [15, 16]. This report will focus on the regime in which the diode behaviours can be well-fitted using the Shockley diode equation.

The curves in figure 2 yielded ideality factors between 1.49 and 1.93, indicating that recombination current dominates in each device at each measured temperature. For these fittings, the strongly temperature-dependent J_0 values were allowed to vary freely, meaning that this fitting only describes the voltage dependence of each diode. By using equation (3), it is possible to fit a diode's voltage and temperature dependence simultaneously with a single ideality factor and the band gap listed in table 1. This approach yields the fittings shown in figure 3.

It is clear that the fitting is most accurate at intermediate voltages. At low voltages the influences of photocurrent and parasitic shunt resistance may be important. At high voltages, the diode behaviours all deviate from the Shockley diode equation. Nonetheless, the large ideality factors are consistent with those derived from figure 2 and indicate that the approximation of recombination-dominated current is reasonable for all of the devices measured at elevated temperatures.

Having quantified the voltage and temperature dependence of each of the diodes in figure 3, the band gap dependence was then investigated. The room temperature J_0 value for each of the diodes is plotted as a function of band gap in figure 4.

The F_{Bi} series in figure 4 follows equation (3) with an n value of approximately 1.69, which is similar to the n values of the individual F_{Bi} series devices in figure 3. This indicates that the temperature, voltage and band gap dependent dark current

behaviour throughout this series can be described by a single ideality factor. The T_{grow} series, on the other hand, shows a significantly faster increase of J_0 with decreasing band gap. The enhanced band gap dependence of the current density may be caused by a reduction of τ at lower growth temperatures—note that higher Bi contents and lower band gaps result from lower growth temperatures in the T_{grow} series. To reconcile the different behaviours of the two series, τ would need to reduce by a factor of approximately 40 between growth temperatures of 405 °C and 355 °C. Previous work has observed a two order of magnitude reduction in electron lifetime with a comparable growth temperature reduction in GaAsBi, albeit at lower absolute growth temperatures [33].

These results suggest that the Bi content of the devices has a negligible impact on their dark current properties. However, as the growth temperature must be reduced to achieve higher Bi contents, an increase in dark currents, beyond that induced by the associated band gap shrinkage, may be expected at higher Bi contents. This highlights the importance of growing GaAsBi based devices at an optimised growth temperature in order to achieve the best possible carrier lifetimes and therefore the best possible dark currents. Within the constraints of the low temperatures required for GaAsBi growth, it should be possible to grow high quality devices of arbitrarily high Bi content.

5. Conclusions

The temperature and band gap dependent dark current densities of two series of GaAsBi p-i-n diodes were analysed. The results from devices grown at a common temperature show that recombination current dominates. The devices grown at different temperatures show increased dark current densities associated with lower growth temperatures. This is likely attributable to a reduction in the minority carrier lifetime as has previously been shown to be a result of low temperature growth. The Bi content of the devices appears to have no impact on the device properties other than the resulting band gap reduction causing an associated increase in dark currents.

ORCID iDs

R D Richards ⓘ https://orcid.org/0000-0001-7043-8372
Y Liu ⓘ https://orcid.org/0000-0003-0034-5853
T B O Rockett ⓘ https://orcid.org/0000-0001-8103-0559

References

[1] Sweeney S J and Jin S R 2013 Bismide-nitride alloys: promising for efficient light emitting devices in the near- and mid-infrared *J. Appl. Phys.* **113** 043110

[2] Sweeney S J, Hild K and Jin S 2013 *The potential of GaAsBiN for multi-junction solar cells IEEE 39th Photovoltaic Specialists Conf. (PVSC)* (https://doi.org/10.1109/PVSC.2013.6744977)

[3] Richards R D, Mellor A, Harun F, Cheong J S, Hylton N P, Wilson T, Thomas T, Roberts J S, Ekins-Daukes N J and David J P R 2017 Photovoltaic characterisation of GaAsBi/GaAs multiple quantum well devices *Sol. Energy Mater. Sol. Cells* **172** 238–43

[4] Pursley B, Luengo-Kovac M, Vardar G, Goldman R S and Sih V 2013 Spin lifetime measurements in GaAsBi thin films *Appl. Phys. Lett.* **102** 022420–3

[5] Arlauskas A, Svidovsky P, Bertulis K, Adomavičius R and Krotkus A 2012 GaAsBi photoconductive terahertz detector sensitivity at long excitation wavelengths *Appl. Phys. Express* **5** 022601

[6] Toprasertpong K *et al* 2016 Absorption threshold extended to 1.15 eV using InGaAs/GaAsP quantum wells for over-50%-efficient lattice-matched quad-junction solar cells *Prog. Photovolt., Res. Appl.* **24** 533–42

[7] Alberi K, Dubon O D, Walukiewicz W, Yu K M, Bertulis K and Krotkus A 2007 Valence band anticrossing in GaBi$_x$As$_{1-x}$ *Appl. Phys. Lett.* **91** 051909

[8] Lewis R B, Masnadi-Shirazi M and Tiedje T 2012 Growth of high Bi concentration GaAs$_{1-x}$Bi$_x$ by molecular beam epitaxy *Appl. Phys. Lett.* **101** 082112–5

[9] Dagnelund D, Puustinen J, Guina M, Chen W M and Buyanova I A 2014 Identification of an isolated arsenic antisite defect in GaAsBi *Appl. Phys. Lett.* **104** 052110

[10] Tait C R, Yan L and Millunchick J M 2018 Spontaneous nanostructure formation in GaAsBi alloys *J. Cryst. Growth* **493** 20–24

[11] Puustinen J, Wu M, Luna E, Schramm A, Laukkanen P, Laitinen M, Sajavaara T and Guina M 2013 Variation of lattice constant and cluster formation in GaAsBi *J. Appl. Phys.* **114** 243504

[12] Hunter C J, Bastiman F, Mohmad A R, Richards R, Ng J S, Sweeney S J and David J P R 2012 Absorption characteristics of GaAs$_{1-x}$Bi$_x$/GaAs Diodes in the near-infrared *IEEE Photonics Technol. Lett.* **24** 2191–4

[13] Zhou Z, Mendes D F, Richards R D, Bastiman F and David J P 2015 Absorption properties of GaAsBi based p–i–n heterojunction diodes *Semicond. Sci. Technol.* **30** 094004

[14] Patil P K, Luna E, Matsuda T, Yamada K, Kamiya K, Ishikawa F and Shimomura S 2017 GaAsBi/GaAs multi-quantum well LED grown by molecular beam epitaxy using a two-substrate-temperature technique *Nanotechnology* **28** 105702

[15] Muhammetgulyyev A, Erbas O G, Kinaci B, Donmez O, Celebi Y G and Erol A 2019 Characterization of a GaAs/GaAsBi *pin* solar cell *Semicond. Sci. Technol.* **34** 085001

[16] Hasegawa S, Kakuyama K, Nishinaka H and Yoshimoto M 2019 PEDOT:PSS/GaAs$_{1-x}$Bi$_x$ organic–inorganic solar cells *Japan. J. Appl. Phys.* **58** 060907

[17] Kakuyama K, Hasegawa S, Nishinaka H and Yoshimoto M 2019 Impact of a small change in growth temperature on the tail states of GaAsBi *J. Appl. Phys.* **126** 045702

[18] Rockett T B O, Richards R D, Gu Y, Harun F, Liu Y, Zhou Z and David J P R 2017 Influence of growth conditions on the structural and opto-electronic quality of GaAsBi *J. Cryst. Growth* **477** 139–43

[19] Lewis R B, Beaton D A, Lu X and Tiedje T 2009 GaAs$_{1-x}$Bi$_x$ light emitting diodes *J. Cryst. Growth* **311** 1872–5

[20] Sandall I C, Bastiman F, White B, Richards R, Mendes D, David J P R and Tan C H 2014 Demonstration of InAsBi photoresponse beyond 3.5 μm *Appl. Phys. Lett.* **104** 171109

[21] Cao Z, Veal T D, Ashwin M J, Dawson K and Sandall I 2019 Influence of annealing on the electrical characteristic of GaSbBi Schottky diodes *J. Appl. Phys.* **126** 053103

[22] Gu Y, Zhang Y G, Chen X Y, Ma Y J, Xi S P, Du B and Li H 2016 Nearly lattice-matched short-wave infrared InGaAsBi detectors on InP *Appl. Phys. Lett.* **108** 032102

[23] Ptak A J, Beaton D A and Mascarenhas A 2012 Growth of BGaAs by molecular-beam epitaxy and the effects of a bismuth surfactant *J. Cryst. Growth* **351** 122–5

[24] Richards R D, Bastiman F, Roberts J S, Beanland R, Walker D and David J P R 2015 MBE grown GaAsBi/GaAs multiple quantum well structures: structural and optical characterization *J. Cryst. Growth* **425** 237–40

[25] Wilson T, Hylton N P, Harada Y, Pearce P, Alonso-Álvarez D, Mellor A, Richards R D, David J P R and Ekins-Daukes N J 2018 Assessing the nature of the distribution of localised states in bulk GaAsBi *Sci. Rep.* **8** 6457

[26] Yoshimoto M, Itoh M, Tominaga Y and Oe K 2013 Quantitative estimation of density of Bi-induced localized states in GaAs$_{1-x}$Bi$_x$ grown by molecular beam epitaxy *J. Cryst. Growth* **378** 73–76

[27] Usman M, Broderick C A, Lindsay A and O'Reilly E P 2011 Tight-binding analysis of the electronic structure of dilute bismide alloys of GaP and GaAs *Phys. Rev.* B **84** 245202

[28] Thomas T, Mellor A, Hylton N P, Führer M, Alonso-Álvarez D, Braun A, Ekins-Daukes N J, David J P R and Sweeney S J 2015 Requirements for a GaAsBi 1 eV sub-cell in a GaAs-based multi-junction solar cell *Semicond. Sci. Technol.* **30** 094010

[29] Mohmad A R, Bastiman F, Hunter C J, Richards R D, Sweeney S J, Ng J S, David J P R and Majlis B Y 2014 Localization effects and band gap of GaAsBi alloys *Phys. Status Solidi* B **251** 1276–81

[30] Richards R D, Bastiman F, Hunter C J, Mendes D F, Mohmad A R, Roberts J S and David J P R 2014 Molecular beam epitaxy growth of GaAsBi using As$_2$ and As$_4$ *J. Cryst. Growth* **390** 120–4

[31] Sze S M 1981 *Physics of Semiconductor Devices* 2nd edn (New York: Wiley)

[32] McIntosh K R, Altermatt P P and Heiser G 2000 Depletion-region recombination in silicon solar cells: when does mDR = 2 *16th European Photovoltaic Solar Energy Conf.* (*Glasgow*)

[33] Pačebutas V, Bertulis K, Dapkus L, Aleksejenko G, Krotkus A, Yu K M and Walukiewicz W 2007 Characterization of low-temperature molecular-beam-epitaxy grown GaBiAs layers *Semicond. Sci. Technol.* **22** 819